

# Generalizing Multi-Objective Search via Objective-Aggregation Functions

Hadar Peer<sup>1</sup>, Eyal Weiss<sup>1</sup>, Ron Alterovitz<sup>2</sup>, Oren Salzman<sup>1</sup>

**Abstract**—Multi-objective search (MOS) has become essential in robotics, as real-world robotic systems need to simultaneously balance multiple, often conflicting objectives. Recent works explore complex interactions between objectives, leading to problem formulations that do not allow the usage of out-of-the-box state-of-the-art MOS algorithms. In this paper, we suggest a generalized problem formulation that optimizes solution objectives via aggregation functions of hidden (search) objectives. We show that our formulation supports the application of standard MOS algorithms, necessitating only to properly extend several core operations to reflect the specific aggregation functions employed. We demonstrate our approach in several diverse robotics planning problems, spanning motion-planning for navigation, manipulation and planning for medical systems under obstacle uncertainty as well as inspection planning, and route planning with different road types. We solve the problems using state-of-the-art MOS algorithms after properly extending their core operations, and provide empirical evidence that they outperform by orders of magnitude the vanilla versions of the algorithms applied to the same problems but without objective aggregation.

## I. INTRODUCTION

Multi-objective search (MOS) [19], [24], [25] has emerged as a fundamental tool in robotics, where systems must simultaneously satisfy diverse and often conflicting objectives. Examples include balancing path efficiency with safety, trading off energy consumption against task completion time, or optimizing accuracy while ensuring robustness to uncertainty. In such settings, the ability to reason over multiple objectives during search is indispensable.

Despite progress in MOS algorithms [11], [18], existing formulations largely assume that objectives can be directly optimized in their raw form. However, recent research has demonstrated that this assumption is restrictive: In many robotics domains, objectives interact in ways that are not efficiently captured by independent optimization [7], [23]. Such interactions yield problem formulations that fall outside the direct applicability of standard MOS algorithms, limiting their effectiveness in realistic robotic planning scenarios.

For instance, consider an application of motion-planning for a robot, in which it is desired to have *short* paths and *safe* paths, where safety is the complement of the risk, which corresponds to the collision probability of the robot with environment obstacles. Recent work introduced the concept of *shadows* [2], which is a probabilistic geometric region that is guaranteed to contain the true position of an obstacle with a specified confidence level. The *obstacle-level uncertainty* models obstacle uncertainty better than the standard and less

realistic point-wise uncertainty. Here the overall safety is quantified through the product of non-collision probabilities with each of the obstacles in the environment. Hence, to compute the safety of a path, one is required to reason about each obstacle *independently*, where taking into account a shadow is done by monitoring the closest point along the path to the obstacle. This introduces interactions between obstacle-level collision risks and overall risk. See Fig. 1 for an illustration.

In MOS variants, as the one described above, the current best approach (see, e.g., [7]) is to cast the problem into standard MOS problems by introducing objectives that are required when considering partial paths but won't be part of the final solution (e.g., the risk of each obstacle in the example above will correspond to one objective). Once all solutions are computed, they can be post-processed (e.g., by aggregating risk among different obstacles in our running example). Unfortunately, the number of objectives required to model an underlying MOS problem may be large and the running time of MOS algorithms may grow exponentially with the number of objectives [20]. Thus, this approach is impractical for many settings, motivating more efficient problem representations.

We present a generalized MOS formulation that addresses the limitations of the approach described. Our key insight is to distinguish between *hidden objectives*, which are incrementally computed during the search process, and *solution objectives*, which are defined through aggregation functions over the hidden objectives. This abstraction enables the representation of a broad class of objective interactions while preserving compatibility with state-of-the-art MOS algorithms. Importantly, we show that only minimal algorithmic modifications are required—specifically, the extension of a small set of core operations to incorporate the aggregation functions.

We evaluate our new formulation in several diverse robotics planning problems, including various problems that require balancing path length and safety under obstacle uncertainty for scenarios inspired by navigation, manipulation and medical robotics. In these problems, the hidden objectives correspond to per-obstacle collision probabilities, which are aggregated to yield a goal objective of total collision probability. We instantiate the formulation in state-of-the-art MOS algorithms and provide empirical evidence that the extended variants outperform their standard counterparts when applied to these problems.

**Contribution.** We present the following contributions: (i) A generalized MOS problem formulation that separates

<sup>1</sup>Technion, Israel Institute of Technology, Haifa, Israel.

<sup>2</sup>University of North Carolina at Chapel Hill, NC, USA.

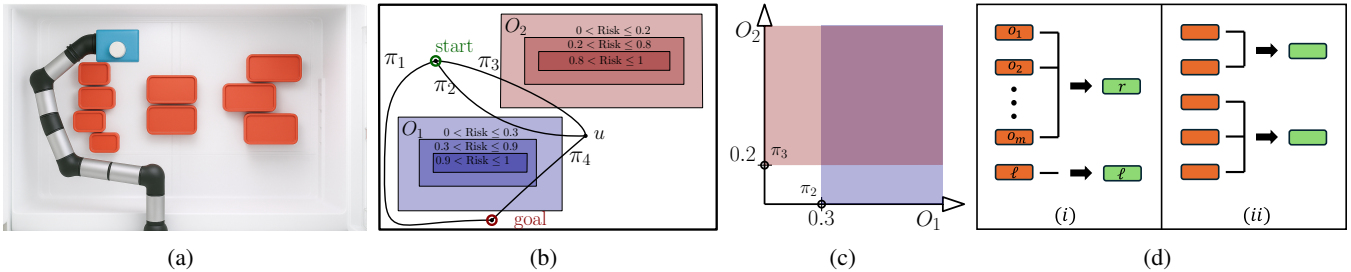


Fig. 1: **Motivating application.** (a) A robot manipulator tasked with grasping a milk carton in a cluttered refrigerator where the precise obstacle location is uncertain. (b) Each obstacle in the configuration space is associated with a shadow, guaranteed to contain its true position with a specified confidence level. Thus, the risk associated with a path corresponds to the “deepest” shadow it intersects. Here, path  $\pi_1$  is guaranteed to be collision free, while paths  $\pi_2, \pi_3, \pi_4$  have maximal collision probabilities of 0.3, 0.2, 0.9, respectively. For  $\pi_2 \cdot \pi_4$  and  $\pi_3 \cdot \pi_4$  (here  $\cdot$  denotes path concatenation), we have maximal collision probabilities of 0.9 and  $1 - (1 - 0.9)(1 - 0.2) = 0.92$ , respectively. When multiple obstacles exist, the risk of each obstacle needs to be accounted for independently. Hence, from start to  $u$ , path  $\pi_2$  has higher risk than  $\pi_3$ , however from start to goal path  $\pi_2 \cdot \pi_4$  has lower risk than  $\pi_3 \cdot \pi_4$ . (c) Pareto-optimal frontier at  $u$ . (d.i) Per-obstacle risks  $o_1, \dots, o_m$  are aggregated into a single risk objective  $r$  (product) and paired with path length objective  $\ell$  to form the bi-objective  $(r, \ell)$ . (d.ii) Example of a different aggregation.

hidden objectives from solution objectives via aggregation functions, enabling the modeling of complex objective interactions. (ii) A demonstration that this formulation supports the application of state-of-the-art MOS algorithms with minimal changes to their core operations. (iii) Empirical evaluation spanning diverse problems depicting the efficacy of using this new formulation when compared to unmodified MOS algorithms.

## II. RELATED WORK

In MOS, formally defined in Sec. III, we aim to compute a set of paths, called the *Pareto-optimal frontier* (POF), that balance the trade-off between a given set of objectives. Namely, the set of paths where no single path is strictly better than the others among all objectives. Exact state-of-the-art algorithms that compute the POF (see e.g., [11], [14], [17], [18]) often build upon the celebrated A\* algorithm [10]. Of particular interest to our work is NAMOA-dr [17] which can handle an arbitrary number of objectives and is used in our evaluation.

In real-world settings we are often not interested in the entire POF—it’s too large to present to decision makers and computationally demanding to compute as the general problem is NP-hard [20]. In such settings, we seek a bounded approximation of the POF, formally defined in Sec. III, which is both small and efficient to compute.

As we outline in Sec. III, there is a simple approach to turning exact MOS algorithms to approximate ones. However, tailored, arguably more complex algorithms exist. They often allow to approximate the POF much faster than the aforementioned simple adaptation. Notable examples include PP-A\* [8] and A\*pex [28]. Their efficiency stems from the observation that paths whose cost is very similar can be grouped in an efficient manner allowing to dramatically prune the POF.

Our work is motivated by recent endeavors that explore complex interactions between objectives in MOS. This in-

cludes a number of papers on lexicographic and hierarchical search, that reflect preferences between objectives, in both deterministic (see e.g., [21] for a single agent motion-planning setting and [29] for a multi-agent setting), and stochastic planning problem setups (see e.g., [15] for heuristic search in stochastic shortest-path and [27] for reward preferences in POMDPs). Other notable directions involve different forms of aggregation, such as scalarizing multi-objective planning using weighted maximization [26], non-additive shortest-path problems [6] and various reformulations of chance-constrained planning (e.g., scenario-based motion-planning [5]). A common theme for all these works is the need to *tailor* algorithmic techniques to fit each new setting. This is addressed by our novel framework, which unifies many problem settings and allows to tackle all of them with the same set of tools.

## III. ALGORITHMIC BACKGROUND

In this section we introduce the notation required to formally define the MOS problem and describe a general algorithmic framework that can be used to solve the problem. For additional details, see e.g. [19], [22].

### A. Notation

Boldface font indicates vectors, lower-case and upper-case symbols indicate elements and sets, respectively. The notation  $p_i$  will be used to denote the  $i$ ’th component of  $\mathbf{p}$ . The addition of two  $d$ -dimensional vectors  $\mathbf{p}$  and  $\mathbf{q}$  and the multiplication of a real-valued scalar  $k$  and a  $d$ -dimensional vector  $\mathbf{p}$  are defined in the natural way, namely as  $\mathbf{p} + \mathbf{q} = (p_1 + q_1, \dots, p_d + q_d)$  and  $k\mathbf{p} = (kp_1, \dots, kp_d)$ , respectively.

Let  $\mathbf{p}$  and  $\mathbf{q}$  be  $d$ -dimensional vectors. For a minimization problem, we say that  $\mathbf{p}$  *dominates*  $\mathbf{q}$  and denote this as  $\mathbf{p} \preceq \mathbf{q}$  if  $\forall i, p_i \leq q_i$ . We say that  $\mathbf{p}$  is *lexicographically smaller* than  $\mathbf{q}$  and denote this as  $\mathbf{p} \prec_{\text{lex}} \mathbf{q}$  if  $p_k < q_k$  for the first index  $k$  s.t.  $p_k \neq q_k$  (or if  $\forall i, p_i \leq q_i$ ). Finally, let  $\mathbf{p}$  and  $\mathbf{q}$  be two  $d$ -dimensional vectors and let  $\varepsilon$  be another

---

**Algorithm 1** MOS-A\*

---

**Input:**  $G = (V, E, \mathbf{c})$ ;  $v_s, v_g$ ;  $\mathbf{h}$

- 1:  $n_{\text{root}} \leftarrow$  new node at  $v_s$  with  $\mathbf{g}(n_{\text{root}}) = \mathbf{0}$ ,  $\mathbf{f}(n_{\text{root}}) = \mathbf{h}(v_s)$
- 2: OPEN.insert( $n_{\text{root}}$ ); SOLS  $\leftarrow \emptyset$ ; CLOSED  $\leftarrow \emptyset$
- 3: **while** OPEN  $\neq \emptyset$  **do**
- 4:  $n \leftarrow$  get\_best\_node(OPEN)
- 5: **if** is\_dominated\_sol( $n$ , SOLS) or  
is\_dominated\_path( $n$ , CLOSED) **then**
- 6:     **continue**
- 7: **if** is\_solution( $n$ ) **then**
- 8:     SOLS.insert( $n$ )
- 9:     **continue**
- 10: **for each**  $v'$  s.t.  $(v(n), v') \in E$  **do**
- 11:      $n' \leftarrow$  new node at  $v'$
- 12:      $\mathbf{g}(n') \leftarrow$  compute\_cost( $\mathbf{g}(n)$ ,  $\mathbf{c}(v(n), v(n'))$ )
- 13:      $\mathbf{f}(n') \leftarrow \mathbf{g}(n') + \mathbf{h}(v')$
- 14:     OPEN.insert( $n'$ )
- 15:     CLOSED.insert( $n$ )
- 16: **return** SOLS

---

**Algorithm 2** MOS-A\* functions (MOS)

---

**function:** get\_best\_node (OPEN)

- 1: **return**  $\arg \min_{\text{lex}} \{ \mathbf{f}(n) \mid n \in \text{OPEN} \}$      /\*  $\mathcal{F}_{\text{agg}}(\mathbf{f}(n))$  \*/

**function:** is\_dominated\_sol ( $n'$ , SOLS)

- 1: **if**  $\exists n \in \text{SOLS}$  s.t.  $\mathbf{f}(n) \preceq \mathbf{f}(n')$  **then** /\*  $\mathcal{F}_{\text{agg}}(\mathbf{f}(n)) \preceq \mathcal{F}_{\text{agg}}(\mathbf{f}(n'))$  \*/
- 2:     **return** true

**function:** is\_dominated\_path ( $n'$ , CLOSED)

- 1: **if**  $\exists n \in \text{CLOSED}$  s.t.  $v(n) = v(n')$  and  $\mathbf{g}(n) \preceq \mathbf{g}(n')$  **then**
- 2:     **return** true

**function:** compute\_cost ( $\mathbf{g}_{\text{parent}}$ ,  $\mathbf{c}$ )

- 1: **return**  $\mathbf{g}_{\text{parent}} + \mathbf{c}$      /\*  $\mathcal{F}_{\text{ext}}(\mathbf{g}_{\text{parent}}, \mathbf{c})$  \*/

---

$d$ -dimensional vector such that  $\forall i \ \varepsilon_i \geq 0$ . We say that  $\mathbf{p}$  *approximately dominates*  $\mathbf{q}$  with an *approximation factor*  $\varepsilon$  and denote this as  $\mathbf{p} \preceq_{\varepsilon} \mathbf{q}$  if  $\forall i, p_i \leq (1 + \varepsilon_i) \cdot q_i$ .

**B. Setting**

A MOS graph  $G$  is a tuple  $(V, E, \mathbf{c})$ , where  $V$  is the finite set of *vertices*,  $E \subseteq V \times V$  is the finite set of *edges*, and  $\mathbf{c} : E \rightarrow \mathbb{R}_{\geq 0}^d$  is a *cost function* that associates a  $d$ -dimensional vector of non-negative real costs with each edge. A *path*  $\pi$  from  $v_1$  to  $v_n$  is a sequence of vertices  $v_1, v_2, \dots, v_n$  such that  $(v_i, v_{i+1}) \in E$  for all  $i \in \{1, \dots, n-1\}$ .

We define the *cost* of a path  $\pi = v_1, \dots, v_n$  as  $\mathbf{c}(\pi) = \sum_{i=1}^{n-1} \mathbf{c}(s_i, s_{i+1})$ . Given paths  $\pi$  and  $\pi'$ , we extend all the above definitions to paths. E.g., we say that  $\pi$  *dominates*  $\pi'$  and denote this as  $\pi \preceq \pi'$  if  $\mathbf{c}(\pi) \preceq \mathbf{c}(\pi')$ .

Let  $G = (V, E, \mathbf{c})$  be a MOS graph and  $v_s, v_g \in V$  start and goal vertices. A path from  $v_s$  to  $v_g$  is called a *solution*. The POF  $\Pi^*$  is the set of all solutions s.t. for every solution  $\pi \in \Pi^*$ , there does not exist a solution  $\pi'$  s.t.  $\pi' \preceq \pi$ .

**C. Algorithms**

Recall (Sec. II) that state-of-the-art MOS algorithms are often A\*-based, thus we restrict our discussion to this family of algorithms (and assume basic familiarity with A\*).

1) *Exact MOS*: Following Skyler et al. [22] we describe in Alg. 1 a simplified A\*-based MOS algorithm. As we shall see shortly, our new formulation will be able to utilize the same

algorithm by surgically replacing key operations. These are highlighted in colored text. For now, we instruct the reader to ignore any text in **magenta**.

We now briefly explain Alg. 1 which runs a best-first search over nodes representing solutions, and utilizes dominance checks to prune dominated solutions that are not part of the POF. In Line 1 the root node and its  $g, f$ -values are initialized according to the start vertex  $v_s$ . In Line 2 the data structures OPEN, CLOSED and SOLS are initialized to include the root node and empty sets respectively. Line 3 loops over the nodes in OPEN until exhaustion, in which SOLS, the POF is returned at Line 16. Line 4 updates the current node  $n$  by removing the best node in OPEN according to the function get\_best\_node, which orders the nodes by lexicographic order of  $f$  values. It is worth noting that utilizing a lexicographic order allows to effectively perform a dimensionality reduction that enhances the node comparison operation (see [17]) and that efficient variants exist (see the overview [19]). Line 5 checks if the node  $n$  is dominated by either a solution which was already found via the function is\_dominated\_sol or by a better path to the node  $n$  via the function is\_dominated\_path. If the node  $n$  is dominated then at Line 6 the node is discarded and the search continues. Line 7 checks if  $n$  is a solution. If true, then it is added to SOLS and the search continues without expanding the node at Lines 8-9. Line 10 loops over the children (neighbors) of  $n$  in the graph  $G$ . After a new child is generated at Line 11, its  $g$ -value is computed at Line 12 using the function compute\_cost. Then, its  $f$ -value is computed at Line 13, and inserted into OPEN at Line 14. After  $n$  is expanded, it is inserted into CLOSED at Line 15.

2) *Approximate MOS*: Recall (Sec. II), that in many real-world settings, we are often interested in a bounded approximation of  $\Pi^*$  which is both small and efficient to compute. To this end, given an approximation factor  $\varepsilon$ , an  $\varepsilon$ -approximate POF  $\Pi_{\varepsilon}^*$  is a set of solutions such that every path in  $\Pi^*$  is  $\varepsilon$ -dominated by a path in  $\Pi_{\varepsilon}^*$ .

A general approach to compute  $\Pi_{\varepsilon}^*$  using an exact MOS algorithm (see e.g., [9]) is to replace the domination test  $\preceq$  used in solution domination (i.e., Line 1 in is\_dominated\_sol) with approximate domination test  $\preceq_{\varepsilon}$ .

**IV. GENERALIZING MOS VIA OBJECTIVE AGGREGATION**

As we will see in Sec. V, many applications do not adhere to the MOS setting described in Sec. III. Roughly speaking, this is because (i) path cost is not necessarily additive and, more importantly, (ii) to compute a final solution, we may need to track multiple objectives for indeterminate nodes. We start by introducing two new functions and use them to generalize the MOS problem (Sec. III). We then continue to describe a straw man algorithm to solve this problem and conclude by introducing a simple-yet-effective adaption to Alg. 1.

**A. Setting**

Let  $G = (V, E, \mathbf{c})$  with  $\mathbf{c} : E \rightarrow \mathbb{R}_{\geq 0}^d$  be a MOS graph. Consider monotonically non-decreasing functions  $\mathcal{F}_{\text{ext}} :$

$\mathbb{R}^m \times \mathbb{R}^d \rightarrow \mathbb{R}^m$  and  $\mathcal{F}_{\text{agg}} : \mathbb{R}^m \rightarrow \mathbb{R}^k$ , denoted as a *path-cost extension function* and an *objective aggregation function*, respectively. We call  $m$  and  $k$  the *hidden objective dimensionality* and *solution objective dimensionality*, respectively.

a) *Path cost*: We generalize the notion of path cost as follows: Given path  $\pi = v_1, \dots, v_n$ , let  $\pi^i = v_1, \dots, v_i$  be the partial path composed of the first  $i$  vertices of  $\pi$  for some  $i \in \{1, \dots, n\}$ . We define the *cost w.r.t. a path-cost extension function* recursively as follows  $\mathbf{c}_{\mathcal{F}_{\text{ext}}}(v_1) := \mathbf{0}$  (vector of zeros with dimension  $m$ ) and for  $i > 1$  we define  $\mathbf{c}_{\mathcal{F}_{\text{ext}}}(\pi^i) := \mathcal{F}_{\text{ext}}(\mathbf{c}_{\mathcal{F}_{\text{ext}}}(\pi^{i-1}), \mathbf{c}(v_{i-1}, v_i))$ .

**Note.** When  $\mathcal{F}_{\text{ext}} := (\mathbf{g}, \mathbf{g}') = \mathbf{g} + \mathbf{g}'$  with  $m = d$ , this is the standard definition of additive path cost. We call such a function a *trivial path-cost extension function*.

b) *Solution cost*: We generalize the notion of the POF as follows: Given a solution  $\pi$ , we define *solution cost w.r.t. an objective-aggregation function* as  $\mathbf{c}_{\mathcal{F}_{\text{agg}}}(\pi) := \mathcal{F}_{\text{agg}}(\mathbf{c}_{\mathcal{F}_{\text{ext}}}(\pi))$ . Similarly, the *POF w.r.t. an objective-aggregation function*  $\Pi_{\mathcal{F}_{\text{agg}}}^*$  is the set of all solutions such that  $\forall \pi \in \Pi_{\mathcal{F}_{\text{agg}}}^*$ , there does not exist a solution  $\pi'$  s.t.  $\mathbf{c}_{\mathcal{F}_{\text{agg}}}(\pi') \prec \mathbf{c}_{\mathcal{F}_{\text{agg}}}(\pi)$ .

**Note.** When  $\mathcal{F}_{\text{agg}}$  is the identity function (and thus  $m = k$ ), this is the standard definition of POF. We call such a function a *trivial objective-aggregation function*.

c) *Examples*: We describe below examples of non-trivial path extension and objective-aggregation functions. As we will see in Sec. V, these model natural robotic applications.

$$\mathcal{F}_{\text{ext}}(\mathbf{c}, \mathbf{c}') = \left( \max(c_1, c'_1), \dots, \max(c_{m-1}, c'_{m-1}), c_m + c'_m \right), \quad (1)$$

$$\mathcal{F}_{\text{agg}}(\mathbf{c}) = \left( 1 - \prod_{i=1}^{m-1} (1 - c_i), c_m \right), \quad (2)$$

$$\mathcal{F}_{\text{agg}}(\mathbf{c}) = \left( (m-1) - \sum_{i=1}^{m-1} c_i, c_m \right). \quad (3)$$

Note that in Eq. (1) it holds that  $m = d$ , and in Equations (2)-(3) we have  $k = 2$ . These aggregations are captured by Fig. 1d.i. Fig. 1d.ii presents a more-general aggregation which, for ease of presentation, are not included here.

## B. Algorithms

Given a MOS problem with a non-trivial path extension function but a trivial objective-aggregation function, we can run almost any MOS algorithm. The only change that is required is updated path cost computation. Returning to our representative MOS algorithm (Alg. 1), this corresponds to updating `compute_cost` to use  $\mathcal{F}_{\text{ext}}$ . This corresponds to replacing the `blue` text in the function with the `magenta` text.

When the objective-aggregation function is non-trivial and we wish to compute  $\Pi_{\mathcal{F}_{\text{agg}}}^*$ , one requires slightly more care. A straw man approach to compute  $\Pi_{\mathcal{F}_{\text{agg}}}^*$  would be to run any MOS algorithm and compute  $\Pi^*$  which corresponds to the POF over the hidden objectives. Then, for every solution

$\pi \in \Pi^*$  compute its solution cost  $\mathbf{c}_{\mathcal{F}_{\text{agg}}}(\pi)$ . Subsequently, we compute the undominated solutions set among these costs.

As the hidden objective dimensionality  $m$  is often much larger than the solution objective dimensionality  $k$ , the size of the POF over the hidden objectives may be much larger than the size of  $\Pi_{\mathcal{F}_{\text{agg}}}^*$  rendering the straw man approach highly inefficient. To this end, we highlight which changes need to be made to our representative MOS algorithm (Alg. 1).

The first change required corresponds to the ordering function of the priority queue OPEN. To employ standard MOS tools such as dimensionality reduction [17], OPEN needs to be ordered lexicographically according to  $\mathcal{F}_{\text{agg}}(\mathbf{f}(n))$  and not lexicographically according to  $\mathbf{f}(n)$ . Returning to Alg. 1, this corresponds to replacing the `blue` text with the `magenta` text in `get_best_node`. This means that the heuristic function  $\mathbf{h}$  should also be computed according to the aggregate cost  $\mathcal{F}_{\text{agg}}$ .

The second change is concerned with domination checks. Since solution cost can't be computed for a node that is not a solution, path domination is performed w.r.t. the hidden objectives (i.e., no changes to function `is_dominated_path`). Solution domination however, can be updated. Here, we simply need to check domination w.r.t.  $\mathcal{F}_{\text{agg}}(\mathbf{f}(n))$ . Again, this corresponds to replacing the `blue` text with the `magenta` text in function `is_dominated_solution`.

To differentiate between the approaches, we denote by  $(k, m)$ -ALG $_{\varepsilon}$  an MOS algorithm ALG together with approximate dominance test  $\varepsilon$  using  $k$  and  $m$  hidden and solution objective dimensionality, respectively. The straw man approach is when  $k = m$ , whereas our proposed objective aggregation corresponds to  $k < m$ .

*Theorem 1:* Let ALG be some MOS algorithm and consider a MOS problem with  $k$  and  $m$  solution and hidden objectives for some  $k < m$ , respectively, and with monotonically non-decreasing path extension and objective-aggregation functions  $\mathcal{F}_{\text{ext}}$  and  $\mathcal{F}_{\text{agg}}$ . If  $(m, m)$ -ALG returns a POF to the MOS problem then  $(k, m)$ -ALG (using the `magenta` text instead of the `blue` text in Alg. 1) also returns a POF to the MOS problem.

Proof omitted due to lack of space<sup>1</sup>. However, it is interesting to note that the monotonicity requirement on  $\mathcal{F}_{\text{ext}}$  can be relaxed, as long as monotonicity is preserved for the solution objectives, defined by  $\mathbf{c}_{\mathcal{F}_{\text{agg}}}(\pi) := \mathcal{F}_{\text{agg}}(\mathbf{c}_{\mathcal{F}_{\text{ext}}}(\pi))$ . We will present such a use case in Sec. V-C.

## V. REPRESENTATIVE APPLICATIONS

### A. Inspection Planning

In robot inspection planning [1], [7] we are given a robot  $\mathcal{R}$  and a set of  $q$  points of interests (POI)  $\mathcal{I} = \{p_1, \dots, p_q\}$ .  $\mathcal{R}$  is equipped with a sensor  $S$  and we are tasked with planning the motion of  $\mathcal{R}$  such that the sensor  $S$  covers as many POIs as possible along its path and minimizes the length of the path. As is common in motion-planning (see, e.g., [16]), some works first sample a roadmap  $G = (V, E)$  (a

<sup>1</sup><https://tinyurl.com/mytheoremproof>

graph embedded in  $\mathcal{R}$ 's configuration space) and solve this discretized problem which is termed the *graph inspection planning* problem.

Interestingly, Fu et al. [7] suggested an algorithm that follows exactly our formulation (though stated in terms that are specific to graph inspection planning) and which inspired the **A\*pex** algorithm. Specifically, each POI  $p_i$  induces a hidden objective  $o_i$  that is set to one if it was sensed somewhere along a path and zero otherwise. Thus, we have here  $m = q + 1$  hidden objectives (one for each POI and one for path length). When extending path  $\pi$  by edge  $e$ , the path extension function (i) sets hidden objective  $o_i$  for  $i \in \{1, \dots, q\}$  to one if it was sensed along  $\pi$  or along  $e$  and (ii) accumulates path length. This is captured exactly by Eq. (1). The final objective is to minimize both the number of POIs that were not seen as well as to minimize the length. This is captured exactly by Eq. (3). Notice that  $c_i, i \in \{1, \dots, m - 1\}$  in both equations are binary variables, s.t.  $c_i \in \{0, 1\}$ . For additional details, see [7].

### B. Planning under Obstacle Uncertainty (OU)

In the problem of planning under obstacle uncertainty (OU), also discussed in Sec. I, we are given a robot  $\mathcal{R}$  operating in workspace  $\mathcal{W}$  consisting of  $q$  obstacles  $\mathcal{O} = \{O_1, \dots, O_q\}$ . The exact location of each obstacle is associated with a probabilistic distribution termed *shadow* [2] (to be formalized shortly) and we are tasked with planning the motion of  $\mathcal{R}$  while minimizing the risk of its path—defined in terms of collision probability with any obstacle in the environment—and its length.

We note that similar problems which build upon shadow formulation such as minimizing collision risk [3] or maintaining risk below a specified threshold [4] were recently introduced. As modeling obstacle uncertainty using shadows is a relatively new concept, for completeness, we formally describe the problem.

A *configuration*  $x$  is a  $t$ -dimensional vector that uniquely identifies the position and orientation of  $\mathcal{R}$  in  $\mathcal{W}$ . The set  $\mathcal{X}$  of all robot configurations is called the *configuration space*. Let  $\text{Shape} : \mathcal{X} \rightarrow 2^{\mathcal{W}}$  be a function that maps each configuration  $x$  to the volume occupied by  $\mathcal{R}$  when placed at  $x$ .

In contrast to standard motion-planning problems, where obstacles are known with certainty, we consider a setting in which obstacles may have uncertain shape, size, or location, modeled using a known distribution: *shadows*.

*Definition 1 (Shadows [2]):* For each obstacle  $O_i \in \mathcal{O}$ , we define a sequence of volumes called *shadows*,  $\mathcal{S}(O_i) = \{S_0^i, S_1^i, \dots\}$ , where  $\forall i, j : S_j^i \subseteq \mathcal{W}, S_j^i \subseteq S_{j+1}^i$ .

Ideally, we would like to utilize the exact collision probability of  $\mathcal{R}$  at  $x$  with an obstacle  $O_i$ . However, we do not assume that we do not have access to it. Instead, let  $r_{\max} : \mathcal{S} \rightarrow [0, 1]$  associate each shadow with an upper bound on the collision probability with its underlying obstacle. Namely, for every configuration  $x$ , we have that,

$$r_{\max}(S_j^i) \geq \text{Prob.}[\text{Shape}(x) \cap O_i \neq \emptyset \mid \text{Shape}(x) \cap S_j^i \neq \emptyset].$$

Then, we define the *shadow's risk* as an upper bound on the collision probability of  $\mathcal{R}$  to intersect shadow  $S_j^i$  of obstacle  $O_i$  when at configuration  $x$  to be  $\text{risk}(x, S_j^i) = r_{\max}(S_j^i)$ . Here, we assume that risk monotonically increases for smaller shadows. Namely, a smaller shadow has a *higher* risk upper bound. Namely,  $\forall i, j, j'$  s.t.  $j < j'$  it holds that  $r_{\max}(S_j^i) > r_{\max}(S_{j'}^i)$ .

Note that the robot may simultaneously intersect several shadows of the same obstacle. Thus, it is useful to define the notion of an *effective shadow* of obstacle  $O_i$  which is the smallest shadow that intersects the robot. Namely, the effective shadow of  $\mathcal{R}$  at configuration  $x$  for obstacle  $O_i$  is defined as  $S_{\text{eff}}^i(x) := S_{\arg \min_j \{j \mid \text{Shape}(x) \cap S_j^i \neq \emptyset\}}$ . Then, an *obstacle's risk*, denoted by  $\text{risk}(x, O_i)$  is the risk of the effective shadow at  $x$ . I.e.,  $\text{risk}(x, O_i) := \text{risk}(x, S_{\text{eff}}^i(x))$ .

A robot's *path*  $\pi : [0, 1] \rightarrow \mathcal{X}$  is a continuous mapping from the interval  $[0, 1]$  into the configuration space. We define *path obstacle's risk*, denoted by  $\text{risk}(\pi, O_i)$ , as the maximal obstacle risk along the path. Namely,  $\text{risk}(\pi, O_i) := \max_{\alpha \in [0, 1]} \{\text{risk}(\pi(\alpha), O_i)\}$ . To define the risk of a path, we assume that the risk of intersecting the different obstacles is *mutually independent*. Thus, the risk of a path  $\pi$  is defined as  $\text{risk}(\pi) := 1 - \prod_{O_i \in \mathcal{O}} (1 - \text{risk}(\pi, O_i))$ . Examples of effective shadows and path risk are shown in Fig 1b.

As in the inspection planning problem, here we limit the problem to searching over a roadmap  $G = (V, E)$  embedded in  $\mathcal{X}$  given start and target vertices  $v_s, v_t \in V$  that correspond to  $\mathcal{R}$ 's start and target configurations. Set  $\Pi(v_s, v_t)$  be the set of all paths connecting  $v_s$  to  $v_t$  in  $G$ . The *minimum-risk and path length motion-planning* problem calls for computing the POF of paths in  $\Pi(v_s, v_t)$  that are not dominated by any solution with respect to risk and path length.

In terms of the objective aggregation framework, computing all paths in the POF can be done by relating each obstacle  $O_i$  with a hidden objective  $o_i$ , and another hidden objective for the path length. Overall, this results in  $m = q + 1$  hidden objectives. When extending a path  $\pi$  by an edge  $e$ , the path extension function (i) evaluates the obstacle risk per hidden objective  $o_i$  for  $i \in \{1, \dots, q\}$  and (ii) accumulates path length. This is captured by Eq. (1). The solution objectives of minimizing path risk and path length are captured by Eq. (2).

### C. Route Planning with Road Types

In route planning with road types, we are given a ground vehicle  $\mathbb{R}$ , a road network represented as a graph  $G$  with two types of edges corresponding to paved and unpaved roads. Following state-of-the-art navigation applications such as Waze, we are tasked with planning the shortest route while avoiding long unpaved roads. Rephrased as an optimization problem, we aim to minimize both the overall path length and the longest partial path on unpaved roads.

In terms of the objective aggregation framework, this problem can be addressed by defining three hidden objectives:  $g$  for the accumulated road length,  $g_{\text{con}}$  for the consecutive

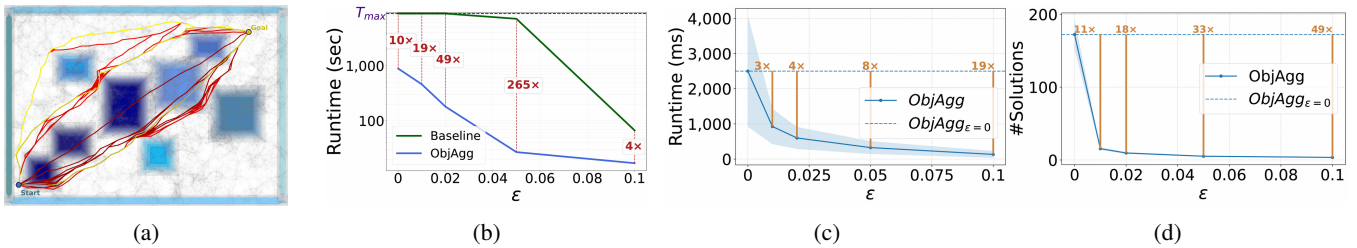


Fig. 2: (a) Point-robot environment together with the roadmap (gray), obstacles with shadows (blue) and one start-goal pair along with all paths in  $\Pi^*$ . (b-d) Performance as a function of the approximation factor  $\epsilon$ , average speedups indicated. (b) Runtimes of **Baseline** and **ObjAgg** shown in log-scale, speedups in red. (c) Runtimes of **ObjAgg** for changing  $\epsilon$  and fixed  $\epsilon = 0$ , speedups in brown. (d) Number of solutions of **ObjAgg** for changing  $\epsilon$  and fixed  $\epsilon = 0$ , speedups in brown.

unpaved road length, and  $g_{\max}$  for the maximal consecutive unpaved road length. The solution objectives in this case are a subset of the hidden objectives:  $g$  and  $g_{\max}$ . The information regarding an edge  $e$  can be encoded by the cost function  $\mathbf{c}$ , which returns a tuple  $(\ell, \text{Type}_e)$ , where the former is the road length and the latter is equal to 1 for paved and 0 for unpaved roads. Thus, we obtain the following extension and aggregation functions:

$$\mathcal{F}_{\text{ext}}((g, g_{\text{con}}, g_{\max}), (\ell, \text{Type}_e)) = \quad (4)$$

$$\begin{cases} (g + \ell, g_{\text{con}} + \ell, \max(g_{\text{con}} + \ell, g_{\max})) & \text{if } \text{Type}_e = 0, \\ (g + \ell, 0, g_{\max}) & \text{if } \text{Type}_e = 1. \end{cases}$$

$$\mathcal{F}_{\text{agg}}(g, g_{\text{con}}, g_{\max}) = (g, g_{\max}). \quad (5)$$

Notice that here  $m = 3, d = k = 2$ , and interestingly  $\mathcal{F}_{\text{ext}}$  is only monotonic w.r.t.  $g, g_{\max}$  (a paved edge resets  $g_{\text{con}}$  to 0); Nevertheless, monotonicity is still preserved for the solution objectives. In the empirical evaluation (presented in Sec. VI) we will discuss practical implications of such cases.

## VI. EXPERIMENTS

We empirically demonstrate the efficacy of using objective aggregation, specifically in the context of computing approximations of  $\Pi^*$  when compared to unmodified MOS algorithms. We evaluate our approach on four different problems which simulate planning under obstacle uncertainty (Sec. V-B) and route planning with road types (Sec. V-C). For the former we consider (i) a point robot moving in the plane, (ii) a 5-link planar manipulator and (iii) The Continuum Reconfigurable Incisionless Surgical Parallel (CRISP) [13] robot moving in the inner surface of a pleural cavity.

We use NAMOA-dr as our MOS algorithm  $\text{ALG}^2$ . For simplicity, we use **Baseline** and **ObjAgg** to refer to the straw man algorithm described in Sec. IV-B (i.e., to  $(m, m)\text{-ALG}_\epsilon$ ) and to our proposed objective aggregation framework (i.e., to  $(k, m)\text{-ALG}_\epsilon$  for  $k < m$ ). Algorithms were implemented in C++, and experiments were conducted on Dell Latitude 5411 with 16 GB RAM, Intel i7-10850H (2.70 GHz), and Ubuntu

<sup>2</sup>Importantly, we also evaluated objective aggregation using the  $\text{A}^*\text{pex}$  algorithms. Results omitted in favor of simplicity of the presentation. The implementation will still be available in our open-source repository.

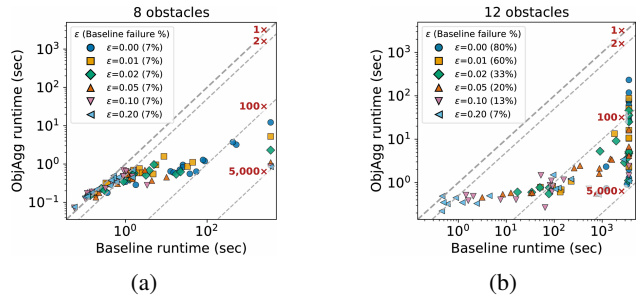


Fig. 3: Point robot log-log scatter plots of runtime (seconds) for **Baseline** (horizontal axis) and **ObjAgg** (vertical axis), for environments with 8, 12 obstacles. Each marker corresponds to a scenario at a given  $\epsilon_{\text{length}}$  value, with consistent color and marker mapping across panels. The diagonal  $1\times$  line indicates equal runtime, and dashed guide lines show speedup factors of  $2\times, 5\times, 100\times,$  and  $5000\times$ . Legends list  $\epsilon$  values for the path length objective together with the percentage of **Baseline** runs that reached the time limit  $T_{\max}$  (failure rate).

18.04.5 LTS. Code, experimental setup and environments will be made publicly available upon paper acceptance.

In all experiments, we use an approximation factor of  $\epsilon \geq 0$  and applied the graph-distance heuristic (i.e., shortest path distances) w.r.t. the path-length objective (or Euclidean distance in C-space in the manipulator environments).

*a) Navigation under OU – Point Robot:* We consider a point robot navigating a 2D environment cluttered with rectangular obstacles. Uncertainty is modeled using Gaussian distributions over the obstacles' widths and heights. For each obstacle, we generated 30 equally-spaced shadows, with each shadow increasing in size by a constant amount. The risk probability of each shadow is evaluated using the corresponding Gaussian distribution. In a preprocessing phase, we generated a roadmap using the PRM algorithm [12] and sampled 20 pairs of vertices whose distance exceeds a minimal threshold, of  $0.6 \cdot d_{\text{env}}$ , where  $d_{\text{env}}$  is the distance between opposite corners in the environment. For each query consisting of a start-goal pair and a value of  $\epsilon$ , we set a timeout of  $T_{\max} = 3600$  seconds. Visualization of the environment and a subset of the POF are provided in Fig. 2a. Here, we have  $m = 13$  hidden objectives, reflecting 12 obstacles and the path length. The experimental results, sum-

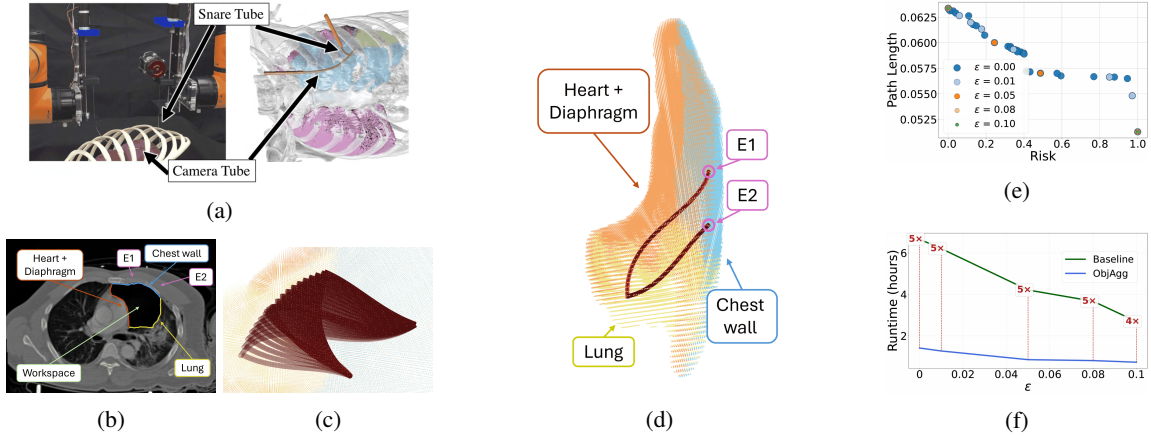


Fig. 4: CRISP robot operating in a lung: (a) Segmented anatomical surfaces with entry points E1 and E2. (b) CT slice visualization. (c) Example of the motion of the CRISP’s tubes. (d) CRISP robotic platform (figure adapted from [7]). (e) Approximate Pareto-optimal frontiers for different  $\epsilon$  values. (f) Runtime of ObjAgg and Baseline as a function of  $\epsilon$ .

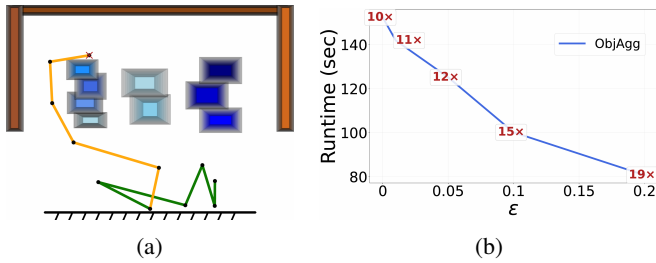


Fig. 5: (a) 5-link manipulator operating in a refrigerator shelf cluttered with obstacles. Initial configuration in green, terminal configuration in orange. (b) Runtime of ObjAgg as a function of increasing  $\epsilon$  and speedups compared to Baseline.

marized in Fig. 2b-2d, demonstrate that ObjAgg significantly outperforms Baseline in terms of runtime, a trend which further intensifies with larger  $\epsilon$  values. Additionally, when  $m$  (number of hidden objectives) increases, the advantage of our aggregation-based method becomes more pronounced, achieving speedups of up to 5000 $\times$  (see Fig. 3).

*b) Manipulation under OU – Planar Manipulator:*

We consider a 5-link manipulator operating in 2D. The setup is motivated by the task of grasping a milk carton on a cluttered refrigerator shelf with rectangular obstacles modeled as boxes (see Fig. 5a). The environment contains 12 obstacles, corresponding to 12 hidden objectives. Uncertainty is represented as Gaussian noise over the obstacle locations. For each of the 12 obstacles, we generated 30 equally-spaced shadows, with each shadow increasing in size by a constant amount. The risk of each shadow is evaluated using the corresponding Gaussian distribution. In a preprocessing phase, a roadmap is generated using the PRM algorithm. We demonstrate the evaluation on a single start–goal configuration task (see Fig. 5a). For this instance, we set a timeout of  $T_{\max} = 1500$  sec. Our algorithm ObjAgg required 152 sec when  $\epsilon = 0$  and 80 sec when  $\epsilon = 0.2$ , while Baseline reached the timeout  $T_{\max}$  for all values of  $\epsilon$ , reflecting speedups of at least 10 – 19 $\times$ .

*c) Manipulation under OU – CRISP robot:* Pleural effusion is a medical condition in which excess fluid accumulates in the pleural cavity, the space between the lungs and the chest wall. To evaluate our method in a clinically motivated setting, we used an anatomical pleural effusion environment derived from a Computed Tomography (CT) scan of a real patient diagnosed with the condition. The internal surface of the cavity is represented as a point cloud, where each point is treated as an obstacle assumed to exist with full certainty. A shadow volume includes all points within a specified distance from an obstacle, and the collision probability with an obstacle is estimated by identifying its innermost shadow, i.e., the smallest distance between the robot and the corresponding obstacle points. Under this uncertainty model, we account for the possibility that the free space available to the robot may shrink, reflecting the uncertainty in pleural effusion anatomy between CT scan acquisition and the medical procedure. For analysis, we segmented the internal surface into three distinct obstacle regions: the lung, the heart and diaphragm (as one obstacle), and the chest wall (excluding the tube entry points). Therefore, in these settings the number of hidden objectives is  $m = 4$ . The environment and CRISP robot are visualized in Fig. 4. As shown in Fig. 4c, the total runtime in the CRISP experiment is significantly higher than in the point robot and manipulator scenarios. This is primarily due to the high computational cost of evaluating the CRISP robot’s shape, making each node expansion much slower. As a representative instance, we consider a task in which the end-effector must move between two distant locations inside the pleural space. In this case, increasing the approximation factor reduces both the number of solutions and the overall runtime. Relative to Baseline, we obtain a speedup of roughly 5 $\times$ .

*d) Route planning with road types:* We used the OpenStreetMap road network of the Boulder Foothills, Colorado, and partitioned the edges into paved and unpaved. From this graph, we sampled 20 source–target pairs whose Euclidean distance is at least 25 km, yielding challenging instances

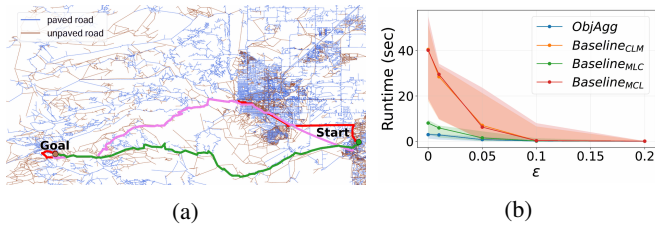


Fig. 6: (a) Road network with road types: paved (blue) and unpaved (brown) with three different paths (green, red, and pink) forming an approximate POF from start to goal. (b) Median runtime as a function of  $\epsilon$ , shaded regions indicate the inter-quartile range (25th–75th percentiles).

with comparable POFs (45+ solutions). Here, the number of hidden objectives is  $m = 3$ . As indicated in Sec. V-C,  $g_{\text{con}}$  is non-monotone and is used by **Baseline** as a solution objective. Thus, the lexicographic order used in **OPEN** matters, as extending nodes by a non-monotonically increasing order may result in the addition of non-optimal solutions to **SOLS**, which implies longer runtimes. Let C, M, L stand for hidden objectives  $g_{\text{con}}, g_{\text{max}}, g_{\ell}$ , respectively. We evaluate three orders: CLM, MLC, and MCL. As shown in Fig. 6b, **ObjAgg** achieves average speedups of 2 $\times$ , 10 $\times$  and 10 $\times$  vs. hidden objective orderings MLC, CLM and MCL, respectively. This provides an insight: **Baseline** is highly sensitive to the lexicographic order used when non-monotone objectives exist, whereas **ObjAgg** is not.

## VII. CONCLUSION AND FUTURE WORK

The objective aggregation framework introduced in this paper offers a unifying abstraction that is both theoretically clean and practically impactful. It allows to naturally model common real-world robotic problems that cannot be efficiently solved using existing MOS machinery. However, despite appearing simple, there are interesting questions that arise: Are there classes of aggregation functions that make the MOS problem provably easier or harder? Are there principled methods for designing admissible and informative heuristics under non-trivial aggregation? Can the framework be extended to richer problem classes? We believe that this paper opens many exciting avenues for future work.

## REFERENCES

- [1] S. D. Alpert, K. Solovey, I. Klein, and O. Salzman. Inspection planning under execution uncertainty. *IEEE Trans. Rob.*, 41:2406–2423, 2025.
- [2] B. Axelrod, L. P. Kaelbling, and T. Lozano-Pérez. Provably safe robot navigation with obstacle uncertainty. *Int. J. of Rob. Res.*, 37(13-14):1760–1774, 2018.
- [3] B. Axelrod and L. Shimanuki. Efficient motion planning under obstacle uncertainty with local dependencies. In *WAFR*, pages 68–84. Springer, 2022.
- [4] C. Dawson, A. Jasour, A. Hofmann, and B. Williams. Provably safe trajectory optimization in the presence of uncertain convex obstacles. In *IROS*, pages 6237–6244, 2020.
- [5] O. de Groot, L. Ferranti, D.M. Gavrilu, and J. Alonso-Mora. Scenario-based motion planning with bounded probability of collision. *Int. J. of Rob. Res.*, 44(9):1507–1525, 2025.
- [6] A. Durand, T. Watteau, G. Ghazi, and R.M. Botez. Generalized shortest path problem: An innovative approach for non-additive problems in conditional weighted graphs. *Mathematics*, 12(19):2995, 2024.

- [7] M. Fu, A. Kuntz, O. Salzman, and R. Alterovitz. Asymptotically optimal inspection planning via efficient near-optimal search on sampled roadmaps. *Int. J. of Rob. Res.*, 42(4-5):150–175, 2023.
- [8] B. Goldin and O. Salzman. Approximate bi-criteria search by efficient representation of subsets of the pareto-optimal frontier. *ICAPS*, 31(1):149–158, 2021.
- [9] B. Goldin and O. Salzman. Approximate bi-criteria search by efficient representation of subsets of the Pareto-optimal frontier. In *ICAPS*, pages 149–158, 2021.
- [10] P. E. Hart, N. J. Nilsson, and B. Raphael. A formal basis for the heuristic determination of minimum cost paths. *IEEE Trans. on Sys. Sci & Cyb.*, 4(2):100–107, 1968.
- [11] C. Hernández, W. Yeoh, Jorge A. Baier, H. Zhang, Luis Suazo, S. Koenig, and O. Salzman. Simple and efficient bi-objective search algorithms via fast dominance checks. *AI*, 314:103807, 2023.
- [12] L. E. Kavradi, P. Svestka, J.C. Latombe, and M.H. Overmars. Probabilistic roadmaps for path planning in high-dimensional configuration spaces. *Trans. on Rob. and Aut.*, 12(4):566–580, 1996.
- [13] A. W. Mahoney, P. L. Anderson, P. J. Swaney, F. Maldonado, and R. J. Webster. Reconfigurable parallel continuum robots for incisionless surgery. In *IROS*, pages 4330–4336, 2016.
- [14] L. Mandow and J.L.P. De La Cruz. Multiobjective A\* search with consistent heuristics. *J. ACM*, 57(5):1–25, 2010.
- [15] S. Miura, K. H. Wray, and S. Zilberstein. Heuristic search for ssps with lexicographic preferences over multiple costs. In *SOCS*, volume 15, pages 127–135, 2022.
- [16] A. Orthey, C. Chamzas, and L. E. Kavradi. Sampling-based motion planning: A comparative review. *Annu. Rev. Control. Robotics Auton. Syst.*, 7(1), 2024.
- [17] F.J. Pulido, L. Mandow, and J.L. Pérez-de-la Cruz. Dimensionality reduction in multiobjective shortest path search. *Comp. & OR*, 64:60–70, 2015.
- [18] Z. Ren, C. Hernández, M. Likhachev, A. Felner, S. Koenig, O. Salzman, S. Rathinam, and H. Choset. EMOA\*: A framework for search-based multi-objective path planning. *AI*, 339:104260, 2025.
- [19] O. Salzman, A. Felner, C. Hernández, H. Zhang, S.-H. Chan, and S. Koenig. Heuristic-search approaches for the multi-objective shortest-path problem: Progress and research opportunities. In *IJCAI*, pages 6759–6768, 2023.
- [20] P. Serafini. Some considerations about computational complexity for multi objective combinatorial problems. In *Recent Advances and Historical Development of Vector Optimization*, pages 222–232. Springer Berlin Heidelberg, 1987.
- [21] T. Shan and B. Englot. A lexicographic search method for multi-objective motion planning. *arXiv preprint arXiv:1909.02184*, 2019.
- [22] S. Skyler, S. S. Shperberg, D. Atzmon, A. Felner, O. Salzman, S.-H. Chan, H. Zhang, S. Koenig, W. Yeoh, and C. Hernández. Theoretical study on multi-objective heuristic search. In *IJCAI*, pages 7021–7028, 2024.
- [23] K. Slutsky, D. S. Yershov, T. Wongpiromsarn, and E. Frazzoli. Hierarchical multiobjective shortest path problems. In *WAFR*, volume 17, pages 261–276, 2021.
- [24] Z. M. Tarapata. Selected multicriteria shortest path problems: An analysis of complexity, models and adaptation of standard algorithms. *Int. J. Appl. Math. Comput. Sci.*, 17(2), 2007.
- [25] EL Ulungu and J Teghem. Multi-objective shortest path problem: A survey. In *Workshop on Multicriteria Decision Making: Methods–Algorithms–Applications*, pages 176–188, 1991.
- [26] N. Wilde, S.L. Smith, and J. Alonso-Mora. Scalarizing multi-objective robot planning problems using weighted maximization. *IEEE Robot. Autom. Lett.*, 9(3):2503–2510, 2024.
- [27] K. Wray, S. Zilberstein, and A.I. Mouaddib. Multi-objective mdps with conditional lexicographic reward preferences. In *AAAI*, volume 29, 2015.
- [28] H. Zhang, O. Salzman, T.K.S. Kumar, A. Felner, C. Hernández, and S. Koenig. A\*pex: efficient approximate multi-objective search on graphs. In *ICAPS*, volume 32, pages 394–403, 2022.
- [29] Z. Zhao, S. Li, S. Liu, M. Zhou, X. Li, and X. Yang. Lexicographic dual-objective path finding in multi-agent systems. *IEEE Trans. on Aut. Sci. & Eng.*, 2024.

## VIII. SUPPLEMENTARY MATERIAL

We restate Thm. 1 and provide a proof for it.

*Theorem 1:* Let ALG be some MOS algorithm and consider a MOS problem with  $k$  and  $m$  solution and hidden objectives for some  $k < m$ , respectively, and with monotonically non-decreasing path extension and objective-aggregation functions  $\mathcal{F}_{\text{ext}}$  and  $\mathcal{F}_{\text{agg}}$ . If  $(m, m)$ -ALG returns a POF to the MOS problem then  $(k, m)$ -ALG (using the magenta text instead of the blue text in Alg. 1) also returns a POF to the MOS problem.

*Proof:* First, note that the lexicographic key used to sort OPEN has no effect on the completeness of the algorithm, as the search terminates only once OPEN turns empty, and paths can only be discarded if they are dominated by a different solution or a different path. Hence, regardless of the order of nodes in OPEN the algorithm  $(k, m)$ -ALG will not terminate before exhausting all possible un-dominated paths.

Second, the `is_dominated_path` is the same as in  $(m, m)$ -ALG, so paths that are not discarded by  $(m, m)$ -ALG are also not discarded by  $(k, m)$ -ALG.

Third, since  $\mathcal{F}_{\text{ext}}$  and  $\mathcal{F}_{\text{agg}}$  are monotonically non-decreasing their composition  $\mathbf{c}_{\mathcal{F}_{\text{agg}}}() := \mathcal{F}_{\text{agg}}(\mathbf{c}_{\mathcal{F}_{\text{ext}}}())$  is also monotonically non-decreasing. Thus,  $\mathbf{g}$  is also monotonically non-decreasing, and given that  $\mathbf{h}$  is admissible (as we assume throughout the paper),  $\mathbf{f}$  is also monotonically non-decreasing. Hence, it holds that paths are encountered in a monotonically non-decreasing order. Namely, solutions that belong to the POF are encountered before non-optimal solutions that do not belong to the POF. Combining this with the fact that  $(k, m)$ -ALG will not terminate before exhausting all possible un-dominated paths (proven above), we can determine that all optimal paths will be found and inserted into SOLS.

Fourth, as `is_dominated_sol` utilizes  $\mathbf{c}_{\mathcal{F}_{\text{agg}}}$  for its domination test, every non-optimal solution (where optimality is w.r.t. the solution objectives) will be discarded if an optimal solution was already found. Combining this with the fact that optimal solutions are guaranteed to be found before their corresponding non-optimal solutions (proven above), we can determine that  $(k, m)$ -ALG returns a POF to the MOS problem defined by the solution objectives. Concluding, if  $(m, m)$ -ALG returns a POF to a MOS problem then  $(k, m)$ -ALG (using the magenta text instead of the blue text in Alg. 1) also returns a POF to its MOS problem. ■